Determination of the parameters affecting electrospun chitosan fiber size distribution and morphology

V. Sencadas[1]; D. M. Correia[2]; A. Areias[1]; G. Botelho[2]; A. M. Fonseca[2]; I. C. Neves[2]; J. L. Gómez-Ribelles[3,4,5] and S. Lanceros-Mendez[1]

[1] *Centro/Departamento de Física, Universidade do Minho, Campus de Gualtar, 4710-058 Braga, Portugal*

[2] *Dept. Química, Centro de Química, Universidade do Minho, Campus de Gualtar, 4710-057 Braga, Portugal;*

[3] *Centro de Biomateriales e Ingeniería Tisular, Universidad Politécnica de Valencia, Camino de Ver s/n, 46022 Valencia, Spain*

[4] *Centro de Investigación Príncipe Felipe, Autopista del Saler 16, 46013 Valencia, Spain*

[5] *CIBER en Bioingeniería, Biomateriales y Nanomedicina, Valencia, Spain*

*e-mail: vsencadas@fisica.uminho.pt

Abstract

The production of chitosan nanofiber mats by electrospinning presents serious difficulties due to the lack of suitable solvents and the strong influence of processing

parameters on the fiber properties. Two are the main problems to be solved: to control the properties of the solution in order to obtain large area uniform fiber mats by having a stable flow rate and to avoid sparks during the process, damaging the fiber mats. In this work chitosan electrospun mats have been prepared form solutions of trifluoroacetic acid / dichloromethane mixtures, allowing to solve the aforementioned problems. Mats with uniform fibers of submicron diameters without beads were obtained. Further, the influence of the different solution and process parameters on the mean fiber diameter and on the width of the distribution of the fiber sizes has been assessed. Solvent composition, needle diameter, applied voltage and traveling distance were the parameters considered in this study.

Introduction

Increasing attention has been given in recent years to natural polymers, such as polysaccharides, due to their abundance in nature, unique structures and characteristics with respect to synthetic polymers (Honarkar & Barikani, 2009). Chitosan is a natural linear polysaccharide composed of glucosamine and N-acetyl glucosamine units linked by β (1-4) glycosidic bonds. Although naturally present in some microorganisms and fungi, commercial chitosan is industrially produced by partial deacetylation of chitin by removal of acetamide groups. Chitin is the second most abundant natural polysaccharide after cellulose. It is mainly found in crustacean shells (shrimp, crab, etc.), insect cuticle and cell walls of fungi (Baldrick, 2010; Fernandez-Megia, Novoa-Carballal, Quiñoá & Riguera, 2005; Krajewska, 2005; Malafaya, Silva & Reis, 2007; Ravi Kumar, 2000). The degree of deacetylation, DD, which defines the distinction between chitin and chitosan, is not precisely established.

45   The term chitosan is found in the literature to describe polymers of chitosan with

46   different molecular weights, viscosity and degree of deacetylation (40-98 %) (Baldrick,

47   2010). However, the term chitosan is generally applied when the degree of deacetylation

48   is above 70 % and the term chitin is used when the degree of deacetylation is below

49   20% (Baldrick, 2010).

50   Chitosan in its crystalline form is usually insoluble in aqueous solutions above a pH of

51   ~7. However, due to the existence of primary amine groups, the structure can be

52   protonated and the protonate free amine groups on glucosamine facilitate the solubility

53   of the molecule, being therefore highly soluble in acid pH (Pillai, Paul & Sharma, 2009;

54   Yaghobi & Hormozi, 2010).

55   Chitosan offers many structural possibilities for chemical modifications in order to

56   induce novel properties, functions and applications, in particular in the biomedical area.

57   It is nontoxic, biocompatible and biodegradable and therefore an excellent material for

58   biomedical applications (Jayakumar, Menon, Manzoor, Nair & Tamura, 2010;

59   Jayakumar, Prabaharan, Nair, Tokura, Tamura & Selvamurugan, 2010; Jayakumar,

60   Prabaharan, Sudheesh Kumar, Nair & Tamura, 2011).

61   Recently, much attention has been paid to chitosan based nanofibers as biomaterial.

62   There are several methods for the fabrication of nanofibers, making use of chemical,

63   thermal and electrostatic principles (Beachley & Wen, 2010). The polymer nanofiber

64   fabrication methods most commonly associated with biomedical applications are

65   electrospinning, self-assembling, peptide reactions and phase separation. The

66   electrospinning process has attracted much attention for the production of polymer

67   fibers as it can produce them with diameters in the range from several micrometers

68   down to tens of nanometers, depending on the polymer and processing conditions

69   (Jayakumar, Prabaharan, Nair & Tamura). The nanofibers produced by this technique

are formed from a liquid polymer solution or melt that is feed through a capillary tube into a region of an electric field generated by connecting a high voltage power source to the capillary tube.

Chitosan nanofibers were successfully prepared by Ohkawa et al. (Ohkawa, Cha, Kim, Nishida & Yamamoto, 2004). The authors studied the solvent effect on the morphology of electrospun chitosan nanofibers by varying chitosan relative concentration with different solvents. The solvents tested were diluted hydrochloric acid, acetic acid, formic acid and trifluoracetic acid (TFA). It was found that when the concentration of chitosan increased, the morphology of the deposited fibers on the collector changed from spherical beads to an interconnected fibrous system. Further, the addition of dichloromethane (DCM) to the chitosan/TFA solution improved the homogeneity of the electrospun chitosan nanofibers. Electrospinning conditions were optimized in order to obtain homogeneous chitosan nanofibers with an average diameter of 330 nm. Other studies on electrospun chitosan nanofibers have been also reported (Jayakumar, Prabaharan, Nair & Tamura). Schiffman et al. obtained bead-free electrospun chitosan nanofibers from a solution of TFA and chitosan with different molecular weights. A small correlation between viscosity and fiber diameter was found (Schiffman & Schauer, 2006, 2007). Despite these efforts, large fiber mats with controlled fiber dimensions are not obtained mainly due to the large electrical conductivity of the TFA solvent, which leads to an unstable process in which the flow rate is controlled by the electric field more than by the dispenser. Further, electrical sparks often occur, damaging parts of the samples. In fact, almost no cell cultures have been reported until now in pure chitosan electrospun fiber mats (Jayakumar, Prabaharan, Nair, Tokura, Tamura & Selvamurugan, 2010; Jayakumar, Prabaharan, Sudheesh Kumar, Nair & Tamura, 2011).

95   The electrospinning technique is very versatile and a wide range of parameters can play

96   an important role in obtaining the desired nanofiber size and microstructure. These

97   parameters include solution viscosity, voltage, feed rate, solution conductivity,

98   capillary-to-collector distance and capillary tube size (Bhardwaj & Kundu; Sill & von

99   Recum, 2008). In this work, a systematic study has been performed in order to solve the

100 aforementioned main problems. By controlling solution parameters a stable process has

101 been achieved allowing obtaining large fiber mats with tailored fiber dimension.

102 Further, the effect of the main processing parameters such as solvent concentration,

103 flow rate, applied voltage, feed rate and inner needle diameter on the chitosan fiber

104 characteristics and sample morphology has been studied in order to set the ground for a

105 systematic and reproducible way to obtain chitosan nanofiber samples for specific

106 applications.

107

108 **Experimental**

109 *Materials*

110 Chitosan practical grade polymer was purchased from Sigma-Aldrich with ≥ 75 %

111 degree of D-acetylation. Dichloromethane (DCM) and Trifluoroacetic acid (TFA, 99 %

112 ReagentPlus) were purchased from Sigma-Aldrich (Table 1). All materials were used as

113 received from the provider.

114

115 **Table 1** – (Budavari, 1996).

116

117

118

119 *Preparation of the solution*

120

121 The polymer was dissolved in a TFA/DCM solution with different TFA/DCM volume

122 ratios for a 7 % (weight) of chitosan. The solution were prepared under a constant and

123 vigorous magnetic stirring (JPSelecta, Agimatic-E) at room temperature until complete

124 dissolution of the chitosan. The viscosity of the prepared solutions was measured in a

125 Viscostar Plus set-up from Fungilab. The variation of the viscosity of the polymer

126 solution with varying TFA/DCM ratio is represented in figure 1.

127

128

129 *Electrospinning*

130 The polymer solution was placed in a commercial plastic syringe fitted with a steel

131 needle. The inner diameter of the needle was 0.5, 1.0 and 1.7 mm for different

132 experiments. Electrospinning was conducted by applying a voltage ranging from 20 and

133 30 kV with a PS/FC30P04 power source from Glassman. A syringe pump

134 (Syringepump) fed the polymer solution into the tip at a rate between 1 and 8 ml.h^{-1}.

135 The electrospun samples were collected on a grounded collecting plate placed at

136 different distances from 50 to 200 mm from the needle tip.

137

138 *Characterization*

139 Electrospun fibers were coated with a thin gold layer using a sputter coater from

140 Polaron (SC502) and the morphology of the membranes were observed by scanning

141 electron microscopy (SEM, JSM-6300 from JEOL) at an accelerating voltage of 15 kV.

142 The fiber diameter distribution was calculated over 50 fibers with the Image J software

143 (J, 2011) from the SEM images obtained at a magnification of 3500 x.

144 The degree of deacetylation was determined by nuclear magnetic ressonance (NMR)

145 according to the procedure described in (Fernandez-Megia, Novoa-Carballal, Quiñoá &

146 Riguera, 2005). Five milligram of chitosan after and before electrospun were added to a

147 5 mm NMR tube containing 0.5 mL of 2 % deutorium chloride (DCl, from Fluka)

148 solution in deuterated water (D_2O, Mw=20,02, ACROS Organics) and heated at 70 °C

149 for 1 h in order to speed up the dissolution. The results for the [1]NMR were collected in a

150 Varian Unity Plus 300 at 70 ºC.

151

152

153 **Results and Discussion**

154

155 Several parameters affect the fiber morphology and size distribution of the polymer

156 electrospun fibers. Among the most important ones are those corresponding to the initial

157 polymer solution: parameters related to the solvent used (dielectric constant, volatility,

158 boiling point and others), the solution concentration (that controls the viscosity) and the

159 molecular weight of the polymer (that allows polymer entanglement). The main

160 parameters that control the jet formation and solvent evaporation rate are the feed rate

161 through the needle and needle diameter, traveling distance from the needle to the

162 collector, temperature and electric field (Ribeiro, Sencadas, Ribelles & Lanceros-

163 Méndez, 2010; S. Ramakrishna, K. Fujihara, W. E. Teo, T. C. Lim & Ma, 2005; Teo &

164 Ramakrishna, 2006).

165 TFA is a strong acid that can dissolve the polymer through the formation of salts that

166 destroy the strong interactions that exist between the molecules of chitosan (Ohkawa,

167 Cha, Kim, Nishida & Yamamoto, 2004). The salt formation occurs between the TFA

168 and the amino groups along the chitosan chain after the following sequential steps: first,

169   protonation of amine groups (-NH$_2$) along the chain of chitosan; second, ionic

170   interaction between protonated amino groups (-NH$_3$) and then formation of

171   trifluoroacetate anions. In this configuration, the salts are soluble in an aqueous media.

172   In this work, solutions of chitosan in TFA/DCM with different relative concentrations

173   were used in order to taylor viscosity and conductivity of the solvent. These parameters

174   have strong influence in the electrospinning process and therefore in the final fiber

175   morphology. The SEM images for the electrospun samples obtained from a solution of

176   chitosan with different TFA/DCM volume ratios and fixed traveling distance of 150

177   mm, needle diameter of 0.5 mm, flow rate of 2 ml.h^{-1} and a voltage of 25 kV are

178   presented in Figure 2.

179   Schiffman et al. reported that electropinning of chitosan in pure TFA solvent was viable

180   for lower chitosan concentrations (2.7 % (w/v)) (Schiffman & Schauer, 2006). In the

181   present work, it was dificult to stabilize the electrospinning process for TFA/DCM

182   concentrations rich in TFA solvent (higher than 80 % TFA) in the solution due to the

183   presence of sparks that frequently appeared during the fiber processing, even for small

184   applied electric fileds, therefore hindering the electrospinning process. An increase of

185   TFA in the solution increases the viscosity (figure 1) and the conductivity of the

186   medium, which are at the origin of the sparks. Electrospinning involves stretching of the

187   solution caused by the repulsion of the charges at its surface. If the conductivity of the

188   solution is increased, more charges can be carried out by the electrospinning jet. The

189   free amines trifluoroacetate anions formed during the chitosan dissolution in TFA

190   increase the conductivity of the solution (Dannhauser & Cole, 1952) and, therefore, the

191   critical voltage for electrospinning to occur is reduced.

192   Further, for TFA/DCM solvent mixtures with low TFA content, the dissolution of the

193   polymer was extremely dificult and during the electrospinning process some drops

194 falled from the needle due to the lower viscosity of the solution, These drops complety

195 dissolved the formed fiber and destroyed the homogenety of the electrospun mats. It

196 was also observed that the average fiber diameter of the electrospun mats decreased

197 with increasing DCM content in the solvent mixture. On the other hand, a larger fiber

198 size distribution was observed with increasing TFA content in the solution a (Figure 3).

199 Figure 3 was obtained from histograms analogous to those shown in Figure 2 (the ones

200 corresponding to Figures 2c and 2d are included in Figure 3), from which the mean

201 value was calculated. The bars in Figure 3 indicate the average and the standard

202 deviation of the fiber diameters.

203 The influence of the inner diameter of the needle in the average size of the electrospun

204 fibers was characterized. For the samples processed with a needle with an inner

205 diameter of 0.5 mm, the presence of very thin fibers with diameters ~ 250 nm was

206 observed. This fact can be attributed to the lower DCM solvent evaporation temperature

207 (Figure 4). On the other hand, the samples obtained with a higher needle diameter show

208 a more uniform fiber size distribution. It was also noted that all samples were free of

209 beads, indicating that the tested chitosan electrospinnig conditions provide sufficient

210 chain entanglement for fiber formation.

211 The presence of small particles (Figure 4b) on the surface of the electrospun fibers has

212 been explained by Zhang et al. as a consequence of the presence of salts (Zhang, Yuan,

213 Wu, Han & Sheng, 2005) originated by the chitosan dissolution in the TFA acid, as

214 explained above. These salts are commonly observed for higher polymer concentrations

215 and higher TFA content in the chitosan-TFA/DCM solvent solution.

216 The average size of the fibers for the different needle inner diameters was calculated

217 and the results show a slight increase of the average fiber diameter from ~ 360 to 410

218 nm with increasing inner needle diameter (figure 5).

219   The fiber diameter distribution along the sample is quite similar for all the electrospun

220   samples, being therefore independent of the needle inner diameter. Literature shows

221   contradictory results in this point. Macossay et al. found no influence of the needle

222   diameter on the average fiber diameter of poly(methyl methacrylate) electrospun fibers

223   (Macossay, Marruffo, Rincon, Eubanks & Kuang, 2007), while Katti et al. and Ribeiro

224   et al. reported that the fiber diameter decreases with decreasing needle inner diameter

225   (Katti, Robinson, Ko & Laurencin, 2004; Ribeiro, Sencadas, Ribelles & Lanceros-

226   Méndez, 2010).

227   A decrease of the inner diameter of the needle causes a reduction of the droplet at the tip

228   and therefore the surface tension of the droplet increases. Then, for a given applied

229   voltage, a larger Coulombic force is required to cause the jet initiation, which results in

230   a decrease of the jet acceleration and, as a consequence, more time is required for the

231   solution to be stretched and elongated before it is collected (S. Ramakrishna, K.

232   Fujihara, W. E. Teo, T. C. Lim & Ma, 2005).

233   The influence of the distance between the needle tip to the grounded collector on the

234   fiber average diameter and distribution was also analyzed. It was observed that the

235   fibers with the smallest average diameter, ~260 nm, were obtained for the samples with

236   a 50 mm distance between needle tip and collector and that the mean fiber diameter

237   increases by increasing the distance between the needle tip and the collector. A

238   maximum average fiber diameter of ~ 500 nm was obtained for a traveling distance of

239   200 mm (Figure 6).

240   It was also observed that the mean diameter fiber distribution increases with increasing

241   the distance between needle tip and sample collector. The presence of sub-structures of

242   smaller fibers between the smooth large fibers (Figure 7) suggests the formation of a

243   secondary jet during the main electrospinning process due to the high solution viscosity

244   (Figure 1). Ding et al. (Ding & et al., 2006) pointed out that this fact is related to certain

245   processing conditions such as high voltage, low relative humidity and fast phase

246   separation of polymer and solvent during the flight between the needle and the collector.

247   Ramakrishna et al. (S. Ramakrishna, K. Fujihara, W. E. Teo, T. C. Lim & Ma, 2005)

248   justified these structures as a consequence of the formations and ejection of smaller jets

249   from the surface of the primary jets, which is comparable to the ejection of the initial jet

250   from the surface of a charged droplet. It was proposed that the elongation of the jet and

251   evaporation of the solvent modifies the shape and the charge density of the jet during

252   the traveling between the tip and the collector. Thus, the balance between the electrical

253   forces and surface tension can change, giving rise to instabilities in the shape of the jet.

254   Such instabilities can decrease the local charge per unit surface area by ejecting a

255   smaller jet from the surface of the primary jet or by splitting apart into two smaller jets.

256   In this work a blend of two solvents with different boiling points (Table 1) has been

257   used and the observed sub-structures of smaller fibers can be related to the fast

258   evaporation of the DCM solvent from the blend during the traveling from the needle tip

259   to the collector, leaving behind solidified fibers with smaller diameters than the ones

260   that crystallize later when the TFA solvent evaporates. This phenomenon was also

261   observed in Figures 2 and 3, when the effect of TFA/DCM solvent ratio on fiber

262   diameter and mat morphology was presented.

263   It is pointed out that an increase of the distance between the tip and the collector often

264   results in a decrease of the fiber diameter (S. Ramakrishna, K. Fujihara, W. E. Teo, T.

265   C. Lim & Ma, 2005). However, in the present work it was observed that the diameter of

266   the fibers increases for increasing distance between the needle tip and the grounded

267   collector. This behavior is to be ascribed to the decrease of the electrostatic field

268 strength resulting in a decrease of the electrostatic force and therefore on the stretching

269 of the fibers.

270 Tip to collector distance has a direct influence on the jet flight time and electric field

271 strength: a decrease of the distance shortens flight and solvent evaporation times and

272 increases the electric field strength. A decrease in the tip-collector distance has a similar

273 effect as increasing the voltage (Figure 8).

274 The changes in the applied electric field have strong influence on the shape of the

275 droplet at the needle tip, its surface charge, dripping rate, velocity of the flowing fluid

276 and hence on the fiber structure and morphology. Similarly, the needle tip to collector

277 distance also determines the time available for fiber drying and the space available for fiber

278 splaying and whipping to take place.

279 The high voltage will induce the necessary charge distribution on the solution and

280 initiate the electrospinning process when the electrostatic force overcomes the surface

281 tension of the solution (S. Ramakrishna, K. Fujihara, W. E. Teo, T. C. Lim & Ma,

282 2005). For higher electric fields, the jet will accelerate and stretch due to the larger

283 Coulombic forces, which results in a reduction of the fiber average diameter and also

284 promotes faster solvent evaporation to yield drier fibers (S. Ramakrishna, K. Fujihara,

285 W. E. Teo, T. C. Lim & Ma, 2005).

286 Finally, the influence of the feed rate on the average fiber distribution was characterized

287 (Figure 9). A minimum value of solution volume suspended at the end of the needle

288 should be maintained in order to form a stable Taylor cone (Teo & Ramakrishna, 2006).

289 The feed rate determines the amount of solution available for the electrospining process.

290 Typically, when the feed rate increases, a corresponding increase of the fiber diameter is

291 observed, as observed i.e. for poly(vinylidene fluoride) (Ribeiro, Sencadas, Ribelles &

292 Lanceros-Méndez, 2010) and for poly(L-lactide acid) (Clarisse & et al., 2011). In

293   chitosan such behavior was not found and the fiber diameter distribution is quite similar

294   for the different feed rates within the range studied in the present work (Figure 9).

295   It was expected that increasing feed rate will increase the volume of the solution drawn

296   from the needle tip, and consequently the jet would take a longer time to dry. The lower

297   boiling point of the solvents used in this work (Table 1) allows the fast evaporation

298   during the flight time. In this situation, full solvent evaporation has already occurred

299   when the fiber reaches the grounded collector and therefore the feed rate does not have

300   influence on the fiber diameter.

301   Most of the physical and chemical properties of this biopolymer strongly depend on the

302   degree of deacetylation (DD) (Lavertu et al., 2003). The DD can be calculated from the

303   ^{1}NMR spectra (figure 10) through:

304

$$DD(\%) = \frac{H_1 D}{H_1 D + \left(\frac{H_{ac}}{3}\right)} \times 100$$

305

306

307   where H_1D is the peak corresponding to the H_1 proton of the deacetylated monomer

308   (duplet at δ= 4.858 ppm) and H_{ac} is the peak of the three protons of the acetyl group

309   (singlet at δ= 1.988 ppm) (Lavertu et al., 2003). The obtained results show that the

310   commercial chitosan has a DD of 78 %, which is similar to the value given by the

311   producer and also similar to the values obtained for the electrospun fibers. It is therefore

312   concluded that the electrospinning process does not affect the degree of deacetylation of

313   the polymer.

314

315   **Conclusions**

316 Large chitosan mats with uniform fibers of submicron diameters without beads have

317 been prepared from trifluoroacetic acid / dichloromethane mixture solutions by a stable

318 electrospinnig process. It was observed that an increase of the DCM present in the

319 solvent blend solution produces nanofibers with smaller diameters and narrower

320 diameter distribution. Inclusion of DCM within the TFA solutions modifies solution

321 viscosity and electrical characteristics, leading to a stable flow rate and avoiding spark

322 formation. The inner diameter of the needle and the feed rate does not have influence in

323 the chitosan electrospun fiber diameter. On the other hand, it was observed that a

324 decrease of the distance from the needle tip to the grounded collector gives origin to

325 nanofibers with smaller diameters. Finally, an increase of the applied voltage also

326 decreases the nanofibers diameter. The degree of deacetylation of the polymer is not

327 affected by the electrospinning process.

328

329

330 **Acknowledgements**

345

References

347 Baldrick, P. (2010). The safety of chitosan as a pharmaceutical excipient. *Regulatory*

348 *Toxicology and Pharmacology, 56*(3), 290-299.

349 Beachley, V., & Wen, X. (2010). Polymer nanofibrous structures: Fabrication,

350 biofunctionalization, and cell interactions. *Progress in Polymer Science, 35*(7), 868-

351 892.

352 Bhardwaj, N., & Kundu, S. C. Electrospinning: A fascinating fiber fabrication

353 technique. *Biotechnology Advances, 28*(3), 325-347.

354 Budavari, S. (1996). *An Encyclopedia of Chemicals, Drugs, and Biologicals*. New

355 Jersey: Merck & Co.

356 Clarisse, R., & et al. (2011). Tailoring the morphology and crystallinity of poly(L-

357 lactide acid) electrospun membranes. *Science and Technology of Advanced Materials,*

358 *12*(1), 015001.

359 Dannhauser, W., & Cole, R. H. (1952). On the Dielectric Constant of Trifluoroacetic

360 Acid1. *Journal of the American Chemical Society, 74*(23), 6105-6105.

361 Ding, B., & et al. (2006). Formation of novel 2D polymer nanowebs via

362 electrospinning. *Nanotechnology, 17*(15), 3685.

363 Fernandez-Megia, E., Novoa-Carballal, R., Quiñoá, E., & Riguera, R. (2005). Optimal

364 routine conditions for the determination of the degree of acetylation of chitosan by 1H-

365 NMR. *Carbohydrate Polymers, 61*(2), 155-161.

15

366 Honarkar, H., & Barikani, M. (2009). Applications of biopolymers I: chitosan.

367 *Monatshefte Fur Chemie, 140*(12), 1403-1420.

368 J, I. (2011). Image Processing and Analysis in Java available from

369 http://rsbweb.nih.gov/ij/index.html.

370 Jayakumar, R., Menon, D., Manzoor, K., Nair, S. V., & Tamura, H. (2010). Biomedical

371 applications of chitin and chitosan based nanomaterials--A short review. *Carbohydrate*

372 *Polymers, 82*(2), 227-232.

373 Jayakumar, R., Prabaharan, M., Nair, S. V., & Tamura, H. Novel chitin and chitosan

374 nanofibers in biomedical applications. *Biotechnology Advances, 28*(1), 142-150.

375 Jayakumar, R., Prabaharan, M., Nair, S. V., Tokura, S., Tamura, H., & Selvamurugan,

376 N. (2010). Novel carboxymethyl derivatives of chitin and chitosan materials and their

377 biomedical applications. *Progress in Materials Science, 55*(7), 675-709.

378 Jayakumar, R., Prabaharan, M., Sudheesh Kumar, P. T., Nair, S. V., & Tamura, H.

379 (2011). Biomaterials based on chitin and chitosan in wound dressing applications.

380 *Biotechnology Advances, 29*(3), 322-337.

381 Katti, D. S., Robinson, K. W., Ko, F. K., & Laurencin, C. T. (2004). Bioresorbable

382 nanofiber-based systems for wound healing and drug delivery: Optimization of

383 fabrication parameters. *Journal of Biomedical Materials Research Part B: Applied*

384 *Biomaterials, 70B*(2), 286-296.

385 Krajewska, B. (2005). Membrane-based processes performed with use of chitin/chitosan

386 materials. *Separation and Purification Technology, 41*(3), 305-312.

387 Lavertu, M., Xia, Z., Serreqi, A. N., Berrada, M., Rodrigues, A., Wang, D., Buschmann,

388 M. D., & Gupta, A. (2003). A validated 1H NMR method for the determination of the

389 degree of deacetylation of chitosan. *Journal of Pharmaceutical and Biomedical*

390 *Analysis, 32*(6), 1149-1158.

391 Macossay, J., Marruffo, A., Rincon, R., Eubanks, T., & Kuang, A. (2007). Effect of

392 needle diameter on nanofiber diameter and thermal properties of electrospun

393 poly(methyl methacrylate). *Polymers for Advanced Technologies, 18*(3), 180-183.

394 Malafaya, P. B., Silva, G. A., & Reis, R. L. (2007). Natural-origin polymers as carriers

395 and scaffolds for biomolecules and cell delivery in tissue engineering applications.

396 *Advanced Drug Delivery Reviews, 59*(4-5), 207-233.

397 Ohkawa, K., Cha, D., Kim, H., Nishida, A., & Yamamoto, H. (2004). Electrospinning

398 of Chitosan. *Macromolecular Rapid Communications, 25*(18), 1600-1605.

399 Pillai, C. K. S., Paul, W., & Sharma, C. P. (2009). Chitin and chitosan polymers:

400 Chemistry, solubility and fiber formation. *Progress in Polymer Science, 34*(7), 641-678.

401 Ravi Kumar, M. N. V. (2000). A review of chitin and chitosan applications. *Reactive*

402 *and Functional Polymers, 46*(1), 1-27.

403 Ribeiro, C., Sencadas, V., Ribelles, J. L. G., & Lanceros-Méndez, S. (2010). Influence

404 of Processing Conditions on Polymorphism and Nanofiber Morphology of Electroactive

405 Poly(vinylidene fluoride) Electrospun Membranes. *Soft Materials, 8*(3), 274 - 287.

406 S. Ramakrishna, K. Fujihara, W. E. Teo, T. C. Lim, & Ma, Z. (2005). *Introduction to*

407 *electrospinning and nanofibers*. Singapure: World Scientific.

408 Schiffman, J. D., & Schauer, C. L. (2006). Cross-Linking Chitosan Nanofibers.

409 *Biomacromolecules, 8*(2), 594-601.

410 Schiffman, J. D., & Schauer, C. L. (2007). One-Step Electrospinning of Cross-Linked

411 Chitosan Fibers. *Biomacromolecules, 8*(9), 2665-2667.

412 Sill, T. J., & von Recum, H. A. (2008). Electrospinning: Applications in drug delivery

413 and tissue engineering. *Biomaterials, 29*(13), 1989-2006.

414 Teo, W. E., & Ramakrishna, S. (2006). A review on electrospinning design and

415 nanofibre assemblies. *Nanotechnology, 17*(14), R89.

416   Yaghobi, N., & Hormozi, F. (2010). Multistage deacetylation of chitin: Kinetics study.

417   *Carbohydrate Polymers, 81*(4), 892-896.

418   Zhang, C., Yuan, X., Wu, L., Han, Y., & Sheng, J. (2005). Study on morphology of

419   electrospun poly(vinyl alcohol) mats. *European Polymer Journal, 41*(3), 423-432.

420

Figure 1 – Variation of the viscosity of the polymer solution with varying TFA/DCM ratio. The line is just a guide for the eyes.

Figure 2 – Morphology of the chitosan mats for the samples obtained with a 7 % (w/v) polymer solution at a traveling distance of 150 mm, needle diameter of 0.5 mm, flow rate of 2 ml.h^{-1} and a voltage of 25 kV: a) 80:20 and b) 60:40 TFA/DCM (v/v) solution; c) and d) represent the fiber diameter histograms of the corresponding figures.

Figure 3 – Influence of the TFA/DCM volume ratio in the distribution of fiber diameters in the electrospun mats obtained for a 7 % (w/v) chitosan solution at a fixed traveling distance of 150 mm, needle diameter of 0.5 mm, flow rate of 2 ml.h^{-1} and a voltage of 25 kV.

Figure 4 – Morphology of the chitosan mats for the samples obtained for a 7 % (w/v) polymer solution, a 70/30 TFA/DCM solvent solution, a traveling distance of 150 mm, flow rate of 2 ml.h^{-1} and a voltage of 25 kV for needle inner diameters of a) 0.5 mm and b) 1.7 mm; c) and d) represent the fiber diameter histograms of the corresponding figures.

Figure 5 – Influence of the inner diameter of the needle in the average fiber diameter and distribution for the electrospun mats obtained for a 7 % (w/v) chitosan solution, a 70/30 TFA/DCM solvent solution, a traveling distance of 150 mm, flow rate of 2 ml.h^{-1} and a voltage of 25 kV.

Figure 6 – Influence of the traveling distance on the fiber average diameter and distribution in the electrospun mats obtained for a 7 % (w/v) chitosan solution, a 70/30 TFA/DCM solvent solution, a needle inner diameter of 0.5 mm, a flow rate of 2 ml.h^{-1} and a voltage of 25 kV.

453   **Figure 7 –** Morphology of the chitosan mats for the samples obtained for a 7 % (w/v)

454   polymer solution, a 70/30 TFA/DCM solvent solution and a needle diameter of 0.5 mm,

455   at a traveling distance of 150 mm, flow rate of 2 ml.h^{-1} a voltage of 25 kV and a

456   distance between the needle tip to the sample collector of a) 50 mm and b) 200 mm.

457

458

459   **Figure 8 –** Influence of the applied voltage on fiber average diameter and distribution in

460   the electrospun mats obtained for a 7 % (w/v) chitosan solution, a 70/30 TFA/DCM

461   solvent solution, needle inner diameter of 1.7 mm, flow rate of 2 ml.h^{-1} and a traveling

462   distance of 15 cm.

463

464   **Figure 9 –** Influence of the feed rate on the average fiber diameter and distribution of

465   the electrospun mats obtained for a 7 % (w/v) chitosan solution, a 70/30 TFA/DCM

466   solvent solution, needle inner diameter of 0.5 mm, flow rate of 2 ml.h^{-1}, a traveling

467   distance of 15 cm and a 25 kV applied voltage.

468

469   **Figure 10 –** ^{1}H-NMR spectra of electrospun chitosan nanofibers at 70 °C.

470

471   **Table 1** – Properties of the solvents used in the present work [17].

472

473

474

475   Table 1

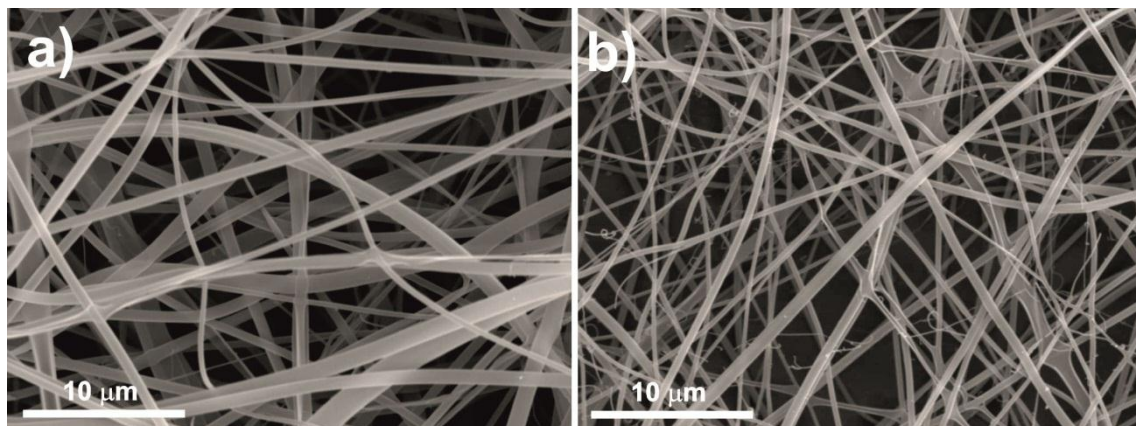| Solvent	Melting Point	Boiling Point	Density	Dipole Moment	Dielectric Constant
	℃	℃	$g.cm^{-3}$	Debye	
TFA	-15.2	73.0	1.535	2.28	8.42
DCM	-95.1	40.0	1.327	1.60	8.93

476
477
478

479   Figure 1
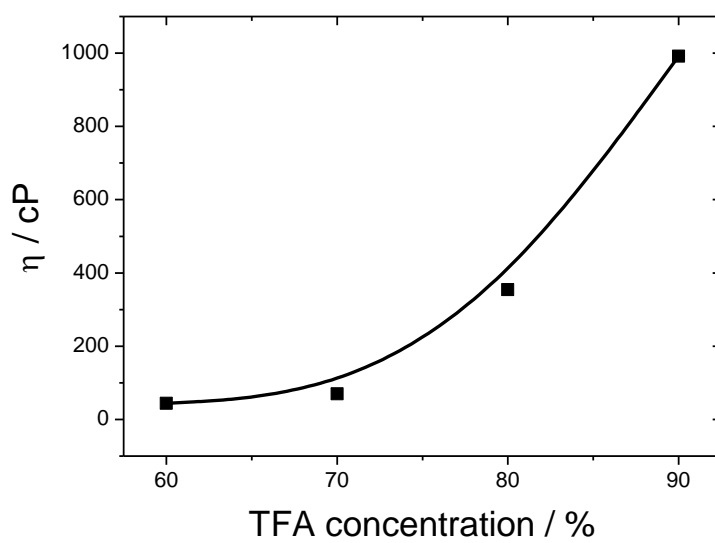
480
481

482   Figure 2

483
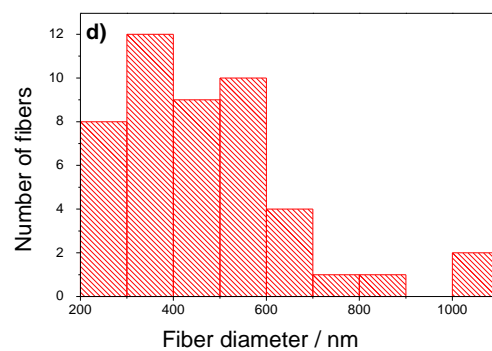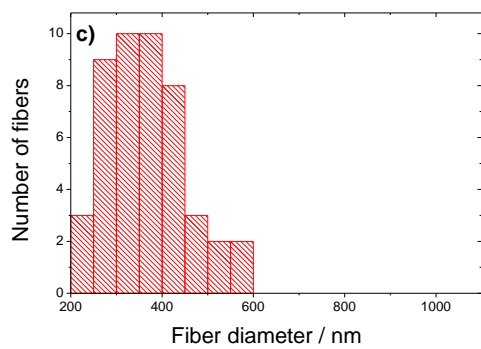
484

485

486   Figure 3
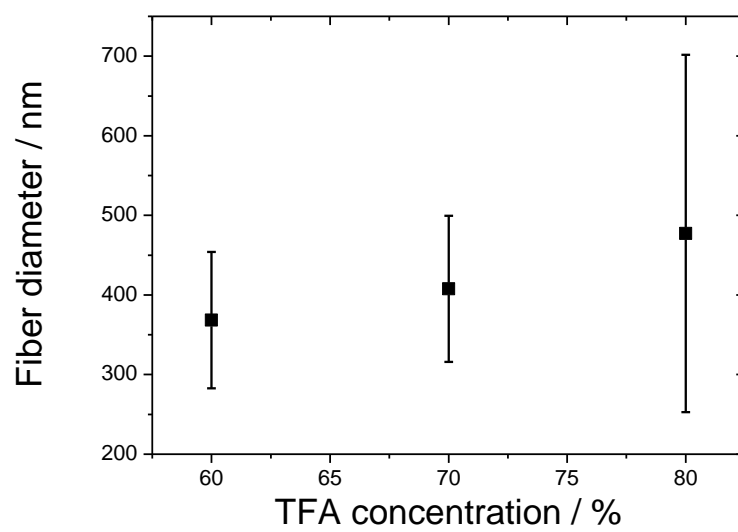
487

488

489   Figure 4
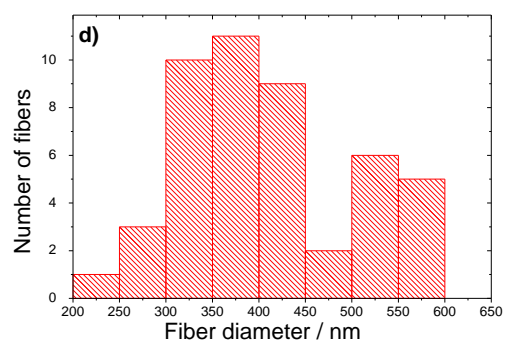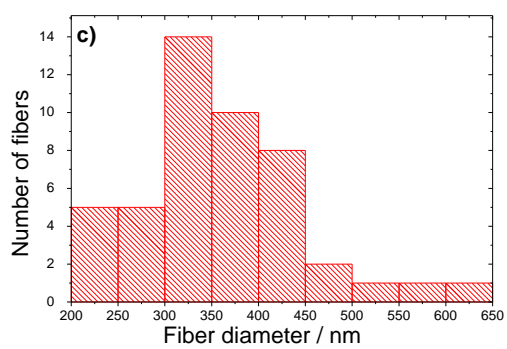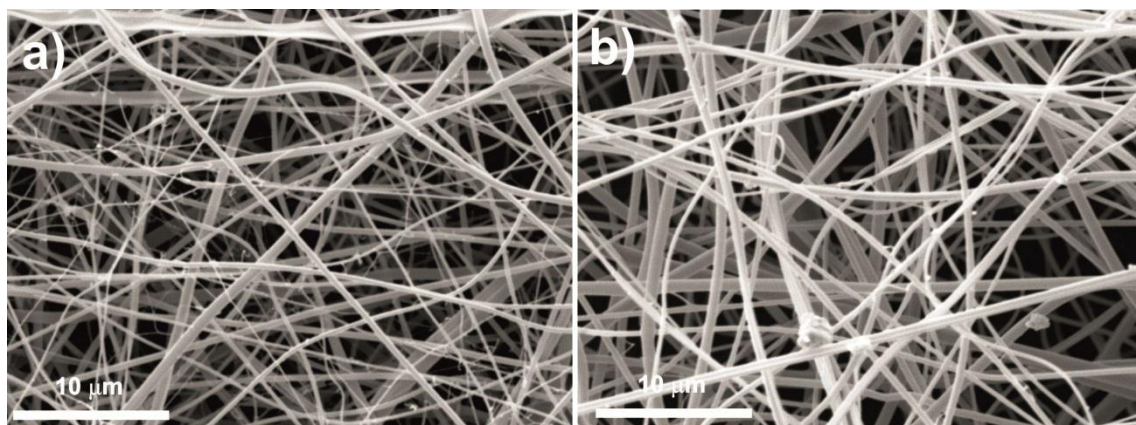
490

491

492   Figure 5
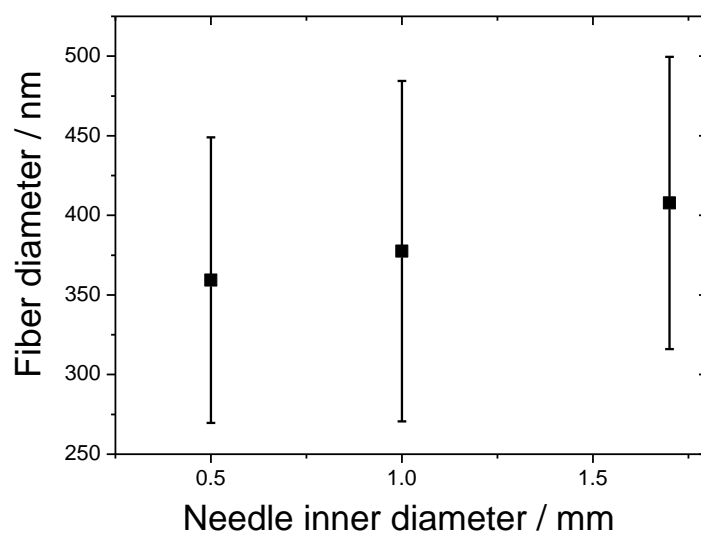
493

494

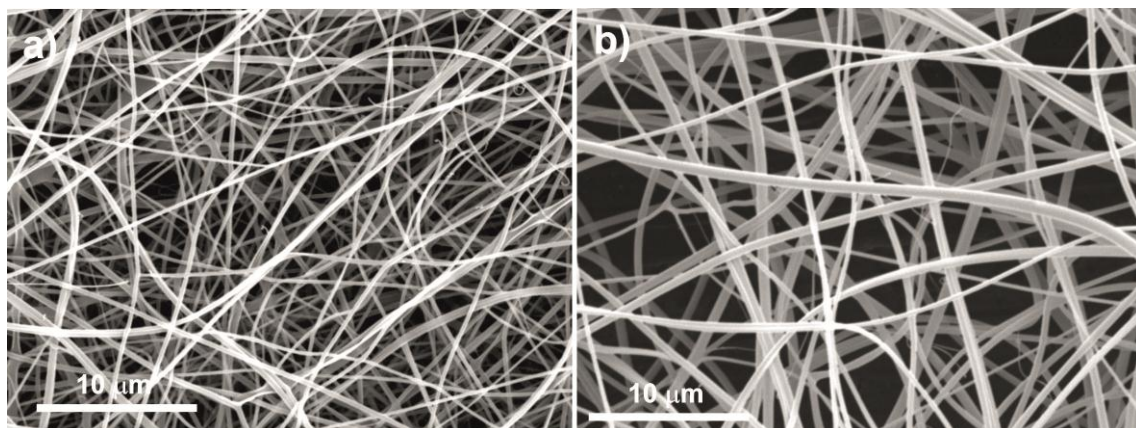495   Figure 6

496
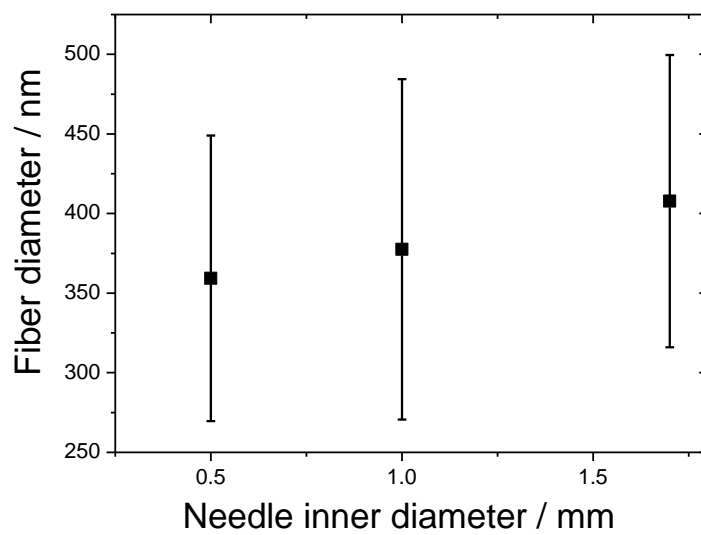
497

498
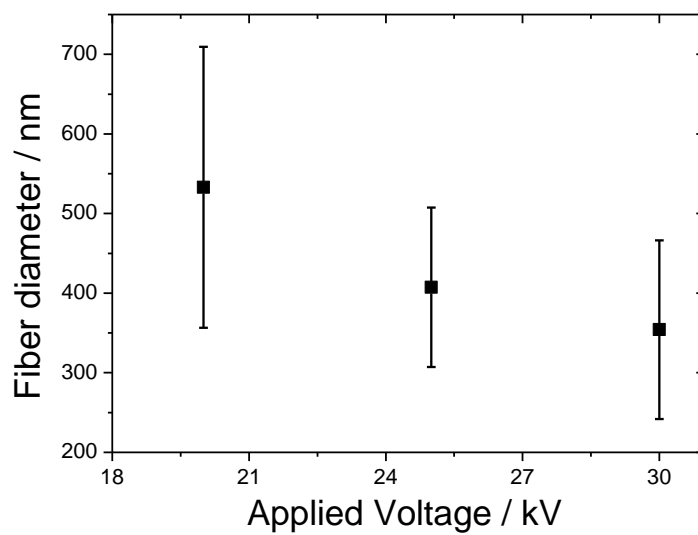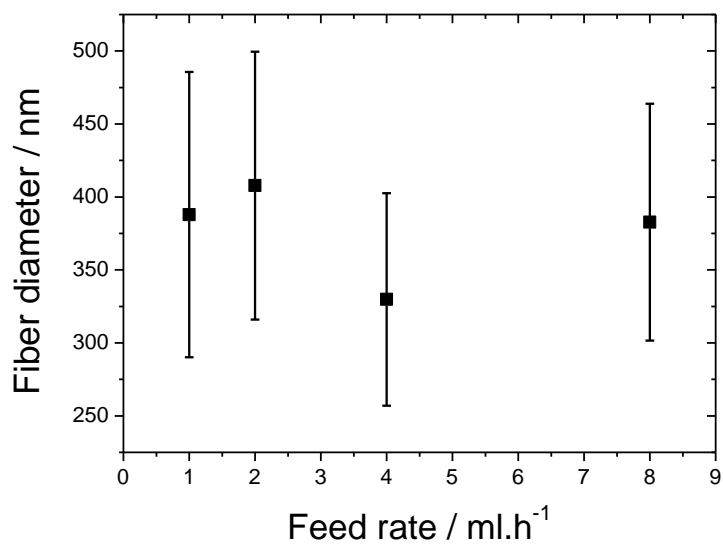
499   Figure 7

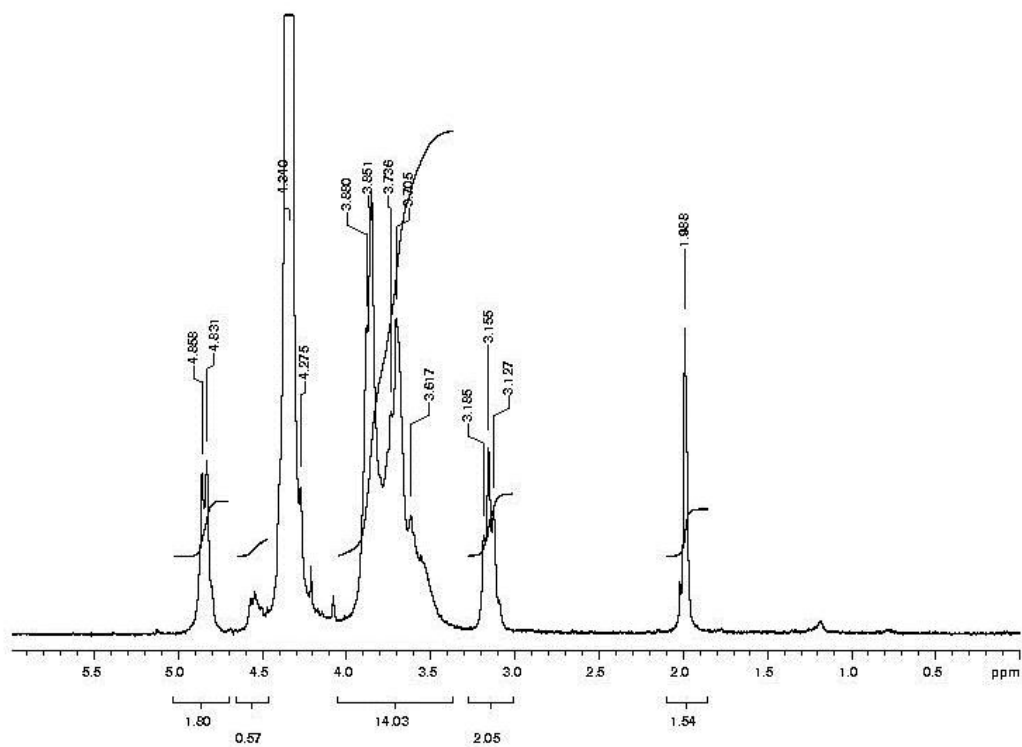500

501
502

503   Figure 8

504

505

506

507   Figure 9

508

509

510

511   Figure 10

512

513
514